

Enhanced energy-constrained quantum communication over bosonic Gaussian channels using multi-channel strategies

Kyungjoo Noh¹, Stefano Pirandola², Liang Jiang³

¹Yale University, ²University of York, ³University of Chicago

April 13, 2020

1 Introduction

Quantum communication is an important branch of quantum information science, promising unconditional security to classical communication and providing the building block of a future large-scale quantum network. Noise in realistic quantum communication channels imposes fundamental limits on the communication rates of various quantum communication tasks. It is therefore crucial to identify or bound the quantum capacities of a quantum channel. In this abstract, we consider **Gaussian thermal channels** that model energy loss and thermal noise errors in realistic optical and microwave communication channels. In particular, we study their various quantum capacities in the energy-constrained scenario to understand the fundamental limits on achievable communication rates with these practically relevant channels.

Our main contribution is to provide **improved lower bounds to various energy-constrained quantum capacities** of the Gaussian thermal channels [1]. That is, we show that higher communication rates can be attained than previously believed. Specifically, we introduce various **multi-channel strategies** and show that they outperform the best known single-channel strategies for the Gaussian thermal channels in the energy-constrained scenarios.

2 Background

Gaussian thermal channels—The Gaussian thermal channel $\mathcal{N}[\eta, \bar{n}_{\text{th}}]$ is defined as the quantum map resulting from applying a beam splitter interaction $\hat{B}(\eta)$ (with a transmissivity $\eta \in [0, 1]$, or loss probability $\gamma = 1 - \eta$) to the joint system of the channel and a thermal environment. The environment is assumed to be initially in a thermal state $\hat{\tau}(\bar{n}_{\text{th}})$, where \bar{n}_{th} is the average photon number and $\hat{\tau}(\bar{n}) \equiv \sum_{n=0}^{\infty} \frac{\bar{n}^n}{(1+\bar{n})^{n+1}} |n\rangle\langle n|$. The beam splitter interaction $\hat{B}(\eta)$ models attenuation of the transmitted quantum signals. Gaussian thermal channels are highly relevant to practically quantum communication scenarios because they are basic models of realistic optical and microwave channels. Especially, added thermal noise (i.e., $\bar{n}_{\text{th}} > 0$) is non-negligible for microwave channels because they are operated at lower frequencies than optical channels. Since the available number of photons is limited in practice, we consider energy-constrained scenarios where each channel can only support at most \bar{n} photons on average.

Best-known energy-constrained strategies for Gaussian thermal channels—Here, we consider three different quantum communication tasks: (1) Quantum state transmission without feedback assistance, (2) quantum state transmission with two-way classical feedback, and (3) secure classical information transmission. For the Gaussian thermal channels, the best-known energy-constrained strategies (before our

work) are to use a single-mode thermal state for the first two tasks [2–4] and to use an ensemble of displaced single-mode thermal states for the last task [5]. Thus, the best-known strategies are **single-channel strategies**. Below, we propose **multi-channel strategies** and demonstrate that they outperform the previously known single-channel strategies in the energy-constrained cases with added thermal noise (i.e., $\bar{n} \leq \infty$ and $\bar{n}_{\text{th}} > 0$).

3 Multi-channel strategies

To deliver the key insight clearly, we focus on the first task, i.e., quantum state transmission without feedback assistance. The achievable communication rate with the best-known single-channel strategy is given by the coherent information of the single-mode thermal state $\hat{\tau}(\bar{n})$ [2]:

$$I_c(\mathcal{N}[\eta, \bar{n}_{\text{th}}], \hat{\tau}(\bar{n})) = g(\eta\bar{n} + (1 - \eta)\bar{n}_{\text{th}}) - g\left(\frac{D + (1 - \eta)(\bar{n} - \bar{n}_{\text{th}}) - 1}{2}\right) - g\left(\frac{D - (1 - \eta)(\bar{n} - \bar{n}_{\text{th}}) - 1}{2}\right). \quad (1)$$

In the special case where there is no added thermal noise (i.e., $\bar{n}_{\text{th}} = 0$), it is proven that this single-channel strategy is optimal [6, 7] (see also Ref. [8]). However, we demonstrate that this is not necessarily the case in the general cases with non-zero added thermal noise (i.e., $\bar{n}_{\text{th}} > 0$). To do so, we introduce **correlated multi-mode thermal states**

$$\hat{\mathcal{T}}(\mathbf{N}, \mathbf{n}) \equiv \hat{U}_{\text{GFT}}^{(N)} \left[\{\hat{\tau}(\bar{n}_1)\}^{\otimes N_1} \otimes \cdots \otimes \{\hat{\tau}(\bar{n}_r)\}^{\otimes N_r} \right] (\hat{U}_{\text{GFT}}^{(N)})^\dagger. \quad (2)$$

Here, $\mathbf{N} = (N_1, \dots, N_r)$ such that $\sum_{k=1}^r N_k = N$ and $\mathbf{n} = (\bar{n}_1, \dots, \bar{n}_r)$. $\hat{U}_{\text{GFT}}^{(N)}$ is the N -mode Gaussian Fourier transformation whose action on the j^{th} annihilation operator \hat{a}_j is defined as $(\hat{U}_{\text{GFT}}^{(N)})^\dagger \hat{a}_j \hat{U}_{\text{GFT}}^{(N)} = \frac{1}{\sqrt{N}} \sum_{k=1}^N e^{i\frac{2\pi}{N}(j-1)(k-1)} \hat{a}_k$. That is, the correlated multi-mode thermal state $\hat{\mathcal{T}}(\mathbf{N}, \mathbf{n})$ is a collection of single-mode thermal states (where each of the first N_1 modes supports on average \bar{n}_1 photons, each of the next N_2 modes supports on average \bar{n}_2 photons and so on) which are uniformly mixed by the Gaussian Fourier transformation $\hat{U}_{\text{GFT}}^{(N)}$ (see Fig. 1(a)). Thus, each mode in the correlated N -mode thermal state $\hat{\mathcal{T}}(\mathbf{N}, \mathbf{n})$ supports on average $\bar{n} = \frac{1}{N} \sum_{k=1}^r N_k \bar{n}_k$ photons. One of our main results is that the following rate is achievable

$$\max_{0 < x \leq 1} x I_c(\mathcal{N}[\eta, \bar{n}_{\text{th}}], \hat{\tau}\left(\frac{\bar{n}}{x}\right)), \quad (3)$$

by using a correlated multi-mode thermal state with $\mathbf{N} = (M, N - M)$ and $\mathbf{n} = (\frac{N}{M}\bar{n}, 0)$ such that $x^* = \frac{M}{N}$. Here, x^* is the optimal x that maximizes the expression in Eq. (3). Note that our strategy is a multi-channel strategy since we use correlated multi-mode thermal states. Moreover, since each channel supports on average \bar{n} photons, the above correlated multi-mode thermal state satisfies the desired energy constraint. Note also that when $x = 1$, our strategy reduces to the previously known single-mode strategy. However, as shown in Fig. 1(b), our multi-channel strategy gives a strictly higher rate than the single-channel strategy when there is a non-zero added thermal noise $\bar{n}_{\text{th}} = 1$. That is, the optimal value of x is strictly less than 1 (see Fig. 1(c)). Thus, **for the first time in the past two decades**, we establish that higher quantum state transmission rates can be achieved with Gaussian thermal channels than previously believed.

The key insight behind the performance boost with our multi-channel strategy is that the coherent information $I_c(\mathcal{N}[\eta, \bar{n}_{\text{th}}], \hat{\tau}(\bar{n}))$ of the single-mode thermal state $\hat{\tau}(\bar{n})$ in Eq. (1) is **convex** in \bar{n} in the small \bar{n} regime when there is non-zero added thermal noise $\bar{n}_{\text{th}} > 0$ in the high loss regime (see the blue line in Fig. 1(d)). Due to the convexity, the achievable region of the single-mode thermal states is strictly contained by its **convex hull** (see the red line and the shaded red region in Fig. 1(d)). Note that in the small \bar{n} regime, the boundary of the convex hull is given by the straight line connecting the origin and the first

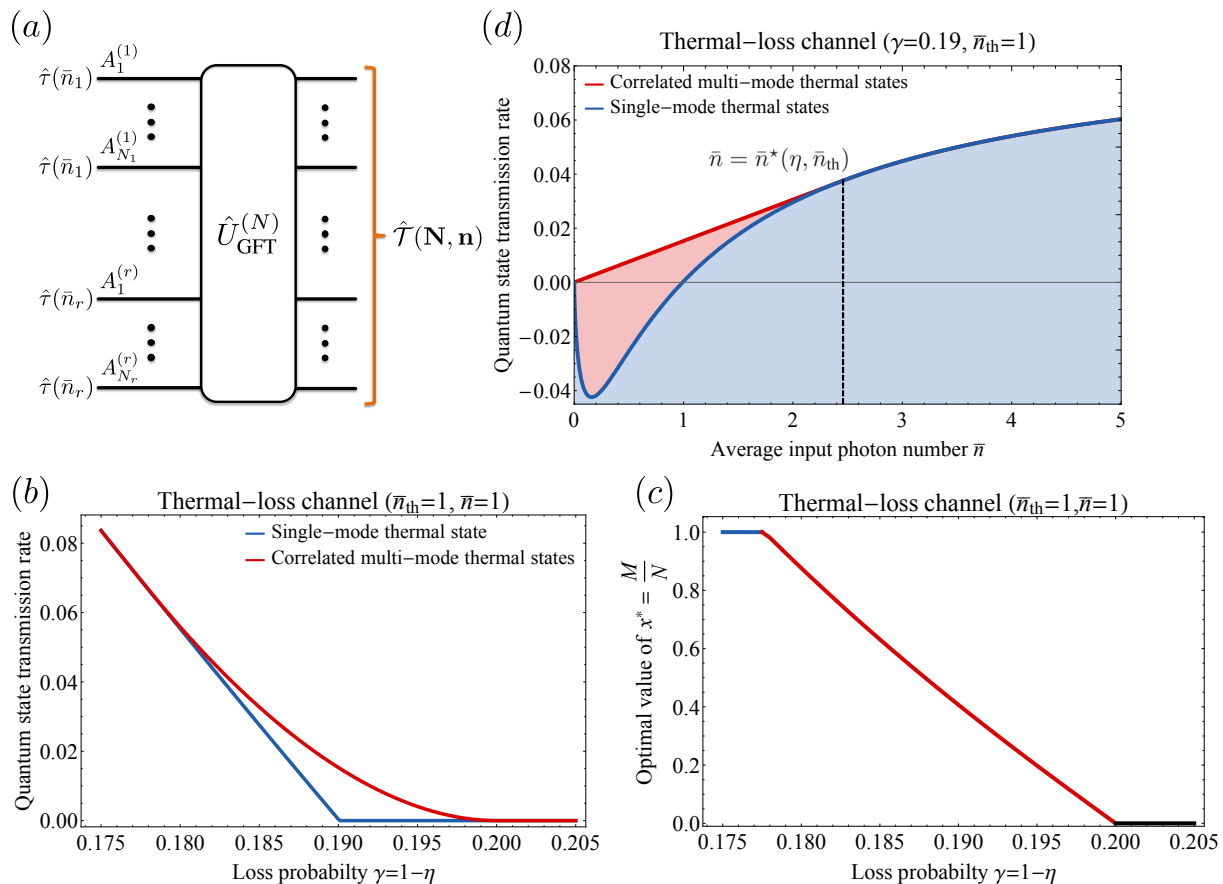


Figure 1: (a) Correlated multi-mode thermal state. (b) Achievable quantum state transmission rate (without feedback assistance) of our multi-channel strategy based on the correlated multi-mode thermal states. (c) The optimal value of x that maximizes the expression in Eq. (3). (d) Coherent information of the single-mode thermal state $\hat{\tau}(\bar{n})$ as a function of the allowed average photon number \bar{n} .

order contact point. Thus, we can understand our multi-channel strategy as a hybridization of the two distinct single-channel strategies, i.e., one with the vacuum state and the other with a thermal state with $\bar{n}^*(\eta, \bar{n}_{\text{th}})$ where the first order contact occurs. Such a hybridization provides a non-trivial advantage when $\bar{n}_{\text{th}} > 0$ since the coherent information is convex. On the other hand, for $\bar{n}_{\text{th}} = 0$, multi-channel strategies are not advantageous since the coherent information is **concave** in \bar{n} for all $\bar{n} \geq 0$.

In the full version of our paper [1], we introduce various other hybridization techniques to boost the achievable rates of the other two communication tasks, i.e., quantum state transmission with two-way classical feedback and secure classical communication. In particular, we show that the two-way-assisted quantum state transmission rate can be significantly improved by **hybridizing forward and backward strategies**, whereas the previous state-of-the-art was to use either a forward or a backward strategy exclusively. We show that the secure classical communication rate can also be improved by using a similar technique given in Fig. 1(d).

Our work is the first to demonstrate that a multi-channel strategy can boost the performance of various communication rates for the practically relevant Gaussian thermal channels. Since the non-trivial advantage is observed in the cases with a non-zero added thermal noise, our results are especially relevant to microwave channels which are corrupted by added thermal noise as well as signal attenuation. Since there have been growing interests in microwave communication (thanks to its compatibility with the superconducting qubit systems) [9, 10], we believe that our work is timely and will have a practical impact in the future, as well as being of fundamental interest.

References

- [1] K. Noh, S. Pirandola, and L. Jiang, “Enhanced energy-constrained quantum communication over bosonic gaussian channels,” *Nature Communications* **11**, 457 (2020).
- [2] A. S. Holevo and R. F. Werner, “Evaluating capacities of bosonic Gaussian channels,” *Phys. Rev. A* **63**, 032312 (2001).
- [3] S. Pirandola, R. García-Patrón, S. L. Braunstein, and S. Lloyd, “Direct and reverse secret-key capacities of a quantum channel,” *Phys. Rev. Lett.* **102**, 050503 (2009).
- [4] R. García-Patrón, S. Pirandola, S. Lloyd, and J. H. Shapiro, “Reverse coherent information,” *Phys. Rev. Lett.* **102**, 210501 (2009).
- [5] K. Sharma, M. M. Wilde, S. Adhikari, and M. Takeoka, “Bounding the energy-constrained quantum and private capacities of phase-insensitive bosonic gaussian channels,” *New Journal of Physics* **20**, 063025 (2018).
- [6] M. M. Wolf, D. Pérez-García, and G. Giedke, “Quantum capacities of bosonic channels,” *Phys. Rev. Lett.* **98**, 130501 (2007).
- [7] M. M. Wilde, P. Hayden, and S. Guha, “Quantum trade-off coding for bosonic communication,” *Phys. Rev. A* **86**, 062306 (2012).
- [8] K. Noh, V. V. Albert, and L. Jiang, “Quantum capacity bounds of gaussian thermal loss channels and achievable rates with gottesman-kitaev-preskill codes,” *IEEE Transactions on Information Theory* **65**, 2563–2582 (2019).
- [9] C. J. Axline, L. D. Burkhardt, W. Pfaff, M. Zhang, K. Chou, P. Campagne-Ibarcq, P. Reinhold, L. Frunzio, S. M. Girvin, L. Jiang, M. H. Devoret, and R. J. Schoelkopf, “On-demand quantum state transfer and entanglement between remote microwave cavity memories,” *Nature Physics* **14**, 705–710 (2018).
- [10] A. J. Wallraff, “Microwave Quantum Network Linking Cryogenic Systems for Superconducting-Circuit-Based Quantum Computing (Conference Presentation),” in *Quantum Technologies 2020*, Vol. 11347, edited by E. Diamanti, S. Ducci, N. Treps, and S. Whitlock, International Society for Optics and Photonics (SPIE, 2020).